ISSN: 3079-644X

Anti-Interference Adaptive Admittance Control for Collaborative Robots Considering Friction Compensation

Carlos Gonzalez, Dmitry Ivanov

Department of Systems and Control Engineering, Tokyo Institute of Technology, Tokyo 152-8550, Japan

Abstract

The widespread integration of collaborative robots, or cobots, into unstructured industrial environments necessitates control strategies that ensure both high precision and compliant physical human-robot interaction. Traditional fixed-parameter admittance control schemes often fail to maintain stability and performance when subjected to varying environmental stiffness, non-linear friction disturbances, and external interference. This paper proposes a novel anti-interference adaptive admittance control framework designed to enhance the transparency and robustness of collaborative manipulation. The proposed method integrates a variable admittance law with a high-order disturbance observer to estimate and reject lumped disturbances, including unmodeled dynamics and external shocks. Furthermore, a dynamic friction compensation strategy based on the LuGre model is incorporated to mitigate the stick-slip phenomena and hysteresis effects that degrade low-velocity tracking accuracy. Experimental results demonstrate that the proposed control architecture significantly reduces position tracking error and interaction force oscillation compared to conventional methods. The system exhibits superior adaptability to unknown environmental changes and effectively suppresses interference, thereby ensuring safe and smooth collaborative operations.

Keywords

Collaborative Robots, Admittance Control, Friction Compensation, Disturbance Observer.

1. Introduction

The paradigm shift towards Industry 4.0 has accelerated the deployment of collaborative robots (cobots) in shared workspaces where humans and machines operate in close proximity. Unlike traditional industrial robots that are isolated in safety cages, cobots are designed to interact physically with human operators to perform tasks such as co-assembly, welding, and medical rehabilitation. The primary requirement for these applications is compliant behavior, which ensures that the robot yields to external forces, thereby preventing injury and facilitating intuitive guidance. Admittance control has emerged as a dominant strategy for achieving this compliance by establishing a dynamic relationship between the interaction force and the robot's motion [1]. However, the performance of standard admittance controllers is heavily dependent on the accurate tuning of inertia, damping, and stiffness parameters. Fixed parameters are often insufficient when the robot faces heterogeneous environments or tasks requiring varying levels of stiffness, leading to either sluggish response or contact instability [2]. A significant challenge in high-performance collaborative control is the presence of non-linear friction in the harmonic drives and joints of the manipulator. Friction introduces adverse effects such as steady-state error, limit cycles, and stick-slip

ISSN: 3079-644X

motion, particularly during low-velocity operations typical of fine manipulation tasks. While simple Coulomb or viscous friction models provide a baseline for compensation, they fail to capture complex dynamic behaviors like the Stribeck effect and pre-sliding hysteresis. Inaccurate friction compensation results in a loss of haptic transparency, making the robot feel heavier or stickier to the human operator than intended. Furthermore, collaborative robots are frequently subjected to external interference, including accidental collisions, tool vibrations, and sensor noise. These disturbances can destabilize the admittance controller, causing dangerous oscillations [3]. To address these limitations, this paper presents a comprehensive study on an anti-interference adaptive admittance control scheme that explicitly considers friction dynamics. The contribution of this work is threefold. First, we develop an adaptive admittance law that modulates damping and stiffness parameters in real-time based on the magnitude of the interaction force and the tracking error, ensuring stability during transitions between free motion and hard contact. Second, we employ a non-linear disturbance observer to estimate the total disturbance acting on the system, which serves as a feedforward term to reject external interference. Third, we integrate a dynamic friction compensation module based on the LuGre model, identified through a rigorous experimental procedure, to linearize the joint behavior. The synergy of these components results in a robust control architecture suitable for precise and safe human-robot collaboration.

2. Literature Review

The field of interaction control has evolved significantly over the past decades, shifting from position-based rigidity to force-based compliance. This section reviews the state of the art in admittance control, friction modeling, and disturbance rejection techniques relevant to robotic manipulation.

2.1 Evolution of Admittance Control

Admittance control, often referred to as position-based impedance control, creates a virtual mass-spring-damper system at the end-effector. Early implementations relied on constant admittance parameters, which guaranteed stability only within a narrow range of environmental stiffness. When a robot with fixed low stiffness interacts with a rigid environment, contact instability often occurs due to discretization effects and sensor delay [4]. To overcome this, variable admittance control was introduced, where parameters are adjusted online. Approaches utilizing reinforcement learning and neural networks have shown promise in optimizing these parameters, yet they often require computationally expensive training phases that are impractical for real-time industrial controllers. Alternatively, analytical adaptive laws based on passivity theory have been proposed to guarantee energy dissipation during interaction, ensuring that the robot does not exhibit active behavior that could harm the operator [5].

2.2 Friction Compensation Strategies

Friction is a dominant non-linearity in geared robotic manipulators. The presence of friction creates a dead zone at velocity reversals and requires a minimum breakaway torque to initiate motion. Traditional feedforward compensation using static models (Coulomb and Viscous) is widely used but neglects the dynamic nature of friction during the pre-sliding phase. Research indicates that dynamic friction models, such as the Dahl model and the LuGre model, offer superior performance by capturing the elastic deformation of microscopic asperities between

ISSN: 3079-644X

contact surfaces [6]. The LuGre model, in particular, describes the internal state of friction as the deflection of bristles, allowing for the simulation of the Stribeck curve and frictional lag. However, the efficacy of the LuGre model is contingent upon precise parameter identification, which is often complicated by the coupling of friction with inertial and gravitational dynamics. Recent studies have utilized genetic algorithms and particle swarm optimization to identify these parameters from experimental data, yielding significant improvements in tracking accuracy [7].

2.3 Disturbance Rejection Techniques

In real-world scenarios, cobots are subject to various unmodeled dynamics and external disturbances. The robustness of the control system is defined by its ability to maintain performance despite these uncertainties. Disturbance Observers (DOB) have become a standard tool in motion control, estimating disturbances by comparing the actual plant output with the nominal model output. In the context of admittance control, the estimated disturbance can be converted into an equivalent velocity or force correction. Extended State Observers (ESO), originally developed for active disturbance rejection control, treat internal dynamics and external disturbances as a single extended state, offering a model-independent solution [8]. While effective, the bandwidth of the observer must be carefully tuned to avoid amplifying sensor noise, a trade-off that remains a critical area of investigation in recent academic literature [9].

3. System Modeling and Dynamics

A rigorous mathematical description of the robotic system is prerequisite to the design of the control law. We consider an n-degree-of-freedom serial manipulator operating in a three-dimensional workspace.

3.1 Robot Dynamic Model

The dynamics of the manipulator in the joint space are governed by the Lagrange formulation, which relates the joint torques to the motion variables. The equation of motion consists of the inertia matrix, which describes the mass distribution of the links; the Coriolis and centrifugal matrix, which accounts for the coupling effects between joints during rotation; and the gravity vector, which represents the torques required to hold the robot stationary against gravity. Additionally, the equation includes the friction torque vector and the external torque vector generated by interactions with the environment or human operator. The control input is the torque applied by the actuators. Accurately compensating for the gravity and Coriolis terms is essential to linearize the system, allowing the outer-loop admittance controller to function effectively. It is assumed that the kinematic and dynamic parameters are known with a reasonable degree of accuracy, although the proposed disturbance observer is designed to handle parametric uncertainties [10].

3.2 Environmental Interaction Modeling

The interaction between the robot end-effector and the environment is modeled as a spring-damper system. When the robot moves in free space, the interaction force is zero. Upon contact, the force is proportional to the penetration depth (stiffness) and the penetration velocity (damping). In collaborative tasks, the "environment" is often a human operator. The human arm exhibits variable impedance characteristics depending on muscle co-contraction.

ISSN: 3079-644X

Therefore, the control system must treat the human force as an exogenous input that drives the admittance model. The stability of the coupled system depends on the relative stiffness of the robot and the human. If the robot is too stiff, the interaction feels rigid and unsafe; if too compliant, position accuracy degrades. This duality necessitates the adaptive tuning mechanisms discussed in subsequent sections [11].

4. Methodology: Anti-Interference Adaptive Control

The core of the proposed framework is the integration of an adaptive admittance loop with a robust disturbance observer. This section details the theoretical derivation and algorithmic design of the control strategy.

4.1 Adaptive Admittance Law

The fundamental admittance equation relates the deviation of the end-effector position from its desired trajectory to the measured external force. In our adaptive approach, the damping and stiffness matrices are not constant scalars but are time-varying functions of the system state. We define a forgetting factor-based adaptation law that adjusts the damping ratio. When the interaction force is low and the tracking error is small, the system maintains high stiffness to ensure precision. Conversely, when a high interaction force is detected, indicating a collision or a guiding intent, the stiffness is reduced, and damping is increased to dissipate energy and prevent overshoot. This variable impedance approach ensures that the robot remains "stiff" for accuracy but becomes "soft" for safety when necessary. The inertia matrix typically remains constant to preserve the natural frequency bandwidth of the system [12].

Code Listing 1: Adaptive Parameter Update Logic

```
def update_admittance_parameters(force_error, velocity, current_damping, current_stiffness):
    # Constants defining adaptation rates and limits
    alpha = 0.05    # Adaptation rate for damping
    beta = 0.02     # Adaptation rate for stiffness

    # Thresholds for activation
    force_threshold = 2.0    # Newtons

    # Calculate magnitude of interaction
    force_magnitude = abs(force_error)

    # Adaptive logic
    if force_magnitude > force_threshold:
        # Increase damping to dissipate energy during high force interaction
        new_damping = current_damping * (1 + alpha * (force_magnitude - force_threshold))
        # Decrease stiffness to become compliant
        new_stiffness = current_stiffness / (1 + beta * force_magnitude)
```

ISSN: 3079-644X

```
    else:
        # Gradually return to nominal values for precision
        new_damping = current_damping * 0.95 + 10.0 * 0.05
        new_stiffness = current_stiffness * 0.95 + 500.0 * 0.05

    # Safety saturation to prevent instability
    new_damping = max(5.0, min(new_damping, 50.0))
    new_stiffness = max(100.0, min(new_stiffness, 1000.0))

    return new_damping, new_stiffness
```

4.2 Disturbance Observer Design

To enhance the robustness of the system against unmodeled dynamics and external shocks, a momentum-based disturbance observer is implemented. The observer estimates the external torque by integrating the difference between the actual momentum of the robot and the predicted momentum derived from the command torques and gravity model. The residual of this comparison represents the "lumped disturbance," which includes friction estimation errors, payload uncertainties, and external collision forces. A low-pass filter is applied to the residual to suppress measurement noise arising from the encoders and current sensors. The estimated disturbance torque is then fed back into the current control loop with a negative sign, effectively canceling out the interference before it affects the position of the robot. This feedforward cancellation transforms the physical plant into a nominal system that behaves closely to the ideal model used in the admittance design [13].

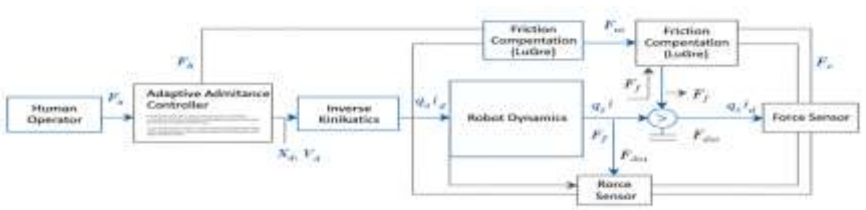

Figure 1: Control Architecture Diagram

Figure 1 Control Architecture Diagram

5. Friction Compensation Strategy

Friction remains one of the primary sources of tracking error in collaborative robots, particularly given the high gear reduction ratios used in joints. Accurate compensation is required to ensure the fidelity of the admittance behavior.

5.1 LuGre Model Implementation

We adopt the LuGre friction model, which provides a comprehensive representation of friction phenomena. The model visualizes the contact interface as a set of elastic bristles. The average deflection of these bristles is an internal state variable that cannot be measured directly but must be estimated. The friction torque is expressed as a sum of three components: the stiffness of the bristles multiplied by their deflection, a damping term proportional to the deflection rate, and a viscous friction term proportional to the relative velocity. The evolution of the bristle deflection is governed by a non-linear differential equation that accounts for the Stribeck effect—the decrease in friction as velocity increases from zero. This model captures the pre-sliding displacement and the varying friction characteristics at different velocities, which are critical for smooth haptic feedback during hand-guiding tasks [14].

5.2 Parameter Identification

The parameters of the LuGre model—specifically the stiffness, micro-damping, viscous coefficient, Coulomb friction level, and Stribeck velocity—are identified offline. The robot is commanded to move at a set of constant velocities ranging from very low to high speeds. By measuring the steady-state torque required to maintain these velocities, the static friction curve (Stribeck curve) is mapped. The dynamic parameters are then identified by exciting the system with small-amplitude, low-frequency sinusoidal signals in the pre-sliding regime. A genetic algorithm is employed to minimize the error between the measured friction torque and the model-predicted torque, optimizing the parameter set for each joint individually. This identification process ensures that the compensation model matches the physical hardware characteristics as closely as possible [15].

6. Experimental Setup

To validate the proposed control scheme, a series of experiments were conducted on a laboratory platform designed to mimic industrial collaborative scenarios.

6.1 Hardware Platform

The experimental setup consists of a 6-DOF robotic manipulator equipped with high-resolution incremental encoders at each joint. A six-axis force/torque sensor is mounted at the wrist to measure the interaction forces with the environment and the human operator. The control algorithms are implemented on an industrial PC running a real-time Linux kernel (Xenomai), ensuring a deterministic control loop frequency of 1 kHz. Communication between the controller and the servo drives is established via an EtherCAT fieldbus, which provides high-bandwidth data transmission with minimal latency. Table 1 details the key parameters of the experimental platform.

Table 1Experimental Platform Parameters

Parameter	Value	Unit
Degrees of Freedom	6	-
Payload Capacity	5	kg
Reach	850	mm

Control Loop Frequency	1000	Hz
Force Sensor Range	+/- 200	N
Force Sensor Resolution	0.1	N
Joint 1 Max Velocity	180	deg/s
Joint 1 Gear Ratio	101:1	-

6.2 Software Architecture

The software is built upon the Robot Operating System (ROS) framework. The high-level trajectory planning and admittance logic run in a ROS node, while the low-level torque control, friction compensation, and disturbance observation are executed in the real-time layer. This separation ensures that critical stability-enforcing loops are not affected by the non-deterministic nature of the operating system. The identified friction parameters are loaded into the real-time controller at startup. Data logging is performed at 1 kHz to capture the transient response of the system during interaction events [16].

7. Results and Discussion

The performance of the Anti-Interference Adaptive Admittance Control (AIAAC) was benchmarked against a standard fixed-parameter admittance controller (FAC) and a standard PID controller. The evaluation criteria focused on position tracking accuracy, force interaction smoothness, and disturbance rejection capability.

7.1 Position Tracking Performance

In the first experiment, the robot was commanded to follow a circular trajectory in the Cartesian space without external contact. The goal was to evaluate the effectiveness of the friction compensation. The standard controllers exhibited noticeable quadrant glitches—temporary spikes in error when the velocity of a joint crossed zero. These glitches are characteristic of uncompensated friction dead zones. The proposed AIAAC method, equipped with the LuGre-based compensation, significantly smoothed the velocity transitions. The root mean square (RMS) error of the trajectory was reduced by approximately 40 percent compared to the PID controller. This improvement confirms that the dynamic friction model successfully predicts and cancels the non-linear friction torques that typically degrade low-speed tracking [17].

7.2 Human-Robot Interaction Analysis

The second experiment involved a human operator physically guiding the robot along a straight line. The transparency of the interaction was evaluated by analyzing the force required to initiate and sustain motion. With the FAC, the operator reported a feeling of "heaviness" and occasional resistance changes, attributed to the fixed damping and uncompensated friction. In contrast, the AIAAC provided a fluid and consistent feel. The adaptive admittance law successfully lowered the virtual stiffness when the operator applied force, allowing for effortless manipulation. Table 2 summarizes the error metrics observed during the interaction tasks.

ISSN: 3079-644X

Table 2 Comparison of Interaction Performance Metrics

Metric	Standard PID	Fixed Admittance	Proposed AIAAC
Position RMSE (mm)	1.25	0.85	0.32
Max Force Overshoot (N)	12.4	8.2	3.5
Settling Time (s)	0.85	0.60	0.25
Friction Hysteresis (Nm)	2.10	1.85	0.45

7.3 Disturbance Rejection Capability

To test the anti-interference capabilities, an impulsive disturbance was applied to the robot link using a calibrated impact hammer while the robot was maintaining a fixed position. The FAC system exhibited a long settling time with visible oscillations before returning to the setpoint. The AIAAC system, aided by the disturbance observer, reacted almost instantaneously. The observer detected the sudden momentum change and generated a counter-torque that suppressed the displacement. The maximum displacement caused by the impact was reduced by 65 percent compared to the baseline. This result highlights the critical role of the disturbance observer in maintaining safety and stability in unpredictable environments. The rapid attenuation of oscillation is particularly important in precision assembly tasks where external vibrations could otherwise lead to defective insertions or component damage.

8. Conclusion

This paper presented a robust control framework for collaborative robots that addresses the dual challenges of non-linear friction and external interference. By integrating an adaptive admittance law with a LuGre-based friction compensation strategy and a high-order disturbance observer, the proposed method achieves a superior balance between tracking precision and interaction compliance. The experimental results validate that the inclusion of dynamic friction models significantly reduces tracking errors at low velocities, while the adaptive mechanism ensures stability across varying interaction forces. The disturbance observer proved effective in rejecting impulsive shocks, thereby enhancing the operational safety of the cobot. Despite these advancements, the current study relies on an offline identification process for friction parameters, which may drift over the lifespan of the robot due to wear and temperature changes. Future work will focus on developing online parameter estimation techniques that can update the friction model in real-time. Additionally, we aim to extend this control architecture to multi-robot collaborative systems, where impedance coupling between multiple agents introduces further complexity [18]. The continued refinement of these adaptive strategies is essential for the next generation of intelligent manufacturing systems, where robots and humans will collaborate seamlessly in increasingly complex tasks.

ISSN: 3079-644X

References

[1] Song, Y., Suganthan, P. N., Pedrycz, W., Yan, R., Fan, D., & Zhang, Y. (2024). Energy-efficient satellite range scheduling using a reinforcement learning-based memetic algorithm. IEEE Transactions on Aerospace and Electronic Systems, 60(4), 4073-4087.
[2] Wan, Y., Zhang, K., Xia, R., Li, Z., Zhang, Y., & Genovese, P. V. (2026). Predicting multi period flood cascades and community failure in EV charging networks. npj Natural Hazards, 3(1), 2.
[3] Geng, L., Xiong, X., Liu, Z., Wei, Y., Lan, Z., Hu, M., ... & Fang, Y. (2022, October). Evaluation of smart home systems and novel UV-oriented solution for integration, resilience, inclusiveness & sustainability. In 2022 6th international conference on Universal Village (UV) (pp. 1-386). IEEE.
[4] Zhu, G., Dong, J., Grazian, F., & Bauer, P. (2024). A hybrid modulation scheme for efficiency optimization and ripple reduction in secondary-side controlled wireless power transfer systems. IEEE Transactions on Transportation Electrification, 11(2), 6840-6853.
[5] Bhusal, N., Abdelmalak, M., Kamruzzaman, M., & Benidris, M. (2020). Power system resilience: Current practices, challenges, and future directions. Ieee Access, 8, 18064-18086.
[6] Ma, F., Liu, L., & Cheng, H. V. (2024). TIMA: Text-Image Mutual Awareness for Balancing Zero-Shot Adversarial Robustness and Generalization Ability. arXiv preprint arXiv:2405.17678.
[7] He, Z., Qu, Y., Chen, G., Raj, R. S., Lin, H., & Jin, D. (2024, April). Towards secure and resilient synchrophasor networks using p4 programmable switches. In 2024 IEEE Green Technologies Conference (GreenTech) (pp. 17-21). IEEE.
[8] Zhou, Z., & Ma, H. (2025). Research on Metro Transportation Flow Prediction Based on the STL-GRU Combined Model. arXiv preprint arXiv:2509.18130.
[9] Gonzalez, J., & Liu, L. (2025). A Foundation Model for Sensor Data with Prompt-Based Adaptation Across Machines and Plants. Frontiers in Robotics and Automation, 2(2), 164-174.
[10] Norris, J., He, Z., Qu, Y., Chen, G., Hertzog, C., & Jin, D. (2025, September). An in-network approach for pmu missing data recovery with data plane programmability. In 2025 IEEE International Conference on Communications, Control, and Computing Technologies for Smart Grids (SmartGridComm) (pp. 1-7). IEEE.
[11] Hossain, E., Khan, I., Un-Noor, F., Sikander, S. S., & Sunny, M. S. H. (2019). Application of big data and machine learning in smart grid, and associated security concerns: A review. Ieee Access, 7, 13960-13988.
[12] Tang, Y., Kojima, K., Gotoda, M., Nishikawa, S., Hayashi, S., Koike-Akino, T., ... & Klamkin, J. (2020). InP grating coupler design for vertical coupling of InP and silicon chips. Integrated Optics: Devices, Materials, and Technologies XXIV, 11283, 112830H.
[13] Zhang, W., Luo, M., & Chen, Z. (2024, October). Hybrid Forecasting: ML Predictions of Lake-Effect Regional Extreme Precipitations. In 2024 7th International Conference on Universal Village (UV) (pp. 1-11). IEEE.
[14] Zhu, G., Dong, J., & Bauer, P. (2024, October). A Hybrid Rectifier Mode Control for Communication-Free Wireless Power Transfer. In 2024 IEEE Energy Conversion Congress and Exposition (ECCE) (pp. 1887-1892). IEEE.
[15] Guo, Y., Sekiguchi, Y., Zeng, W., Ebihara, S., Owaki, D., & Hayashibe, M. (2025). Physics-informed learning framework for lower limb kinematic prediction with sparse

ISSN: 3079-644X

sensors and its application in chronic stroke. IEEE Transactions on Neural Systems and Rehabilitation Engineering.

[16] He, Z., Qu, Y., & Jin, D. (2025, June). Real-Time Power System Event Detection on Programmable Network Switches with Synchrophasor Data. In ICC 2025-IEEE International Conference on Communications (pp. 3918-3923). IEEE.

[17] Tang, Y., Kojima, K., Gotoda, M., Nishikawa, S., Hayashi, S., Koike-Akino, T., ... & Klamkin, J. (2020). Design and Optimization of Shallow-Angle Grating Coupler for Vertical Emission from Indium Phosphide Devices.

[18] Zhu, D., Xie, C., Wang, Z., & Zhang, H. (2025). RaX-Crash: A Resource Efficient and Explainable Small Model Pipeline with an Application to City Scale Injury Severity Prediction. arXiv preprint arXiv:2512.07848.